Active matter transport and jamming on disordered landscapes

C. Reichhardt and C. J. Olson Reichhardt
Theoretical Division, Los Alamos National Laboratory, Los Alamos, New Mexico 87545, USA
(Received 13 February 2014; revised manuscript received 10 June 2014; published 3 July 2014)

We numerically examine the transport of active run-and-tumble particles with steric particle-particle interactions driven with a drift force over random disordered landscapes composed of fixed obstacles. For increasing run lengths, the net particle transport initially increases before reaching a maximum and decreasing at larger run lengths. The transport reduction is associated with the formation of cluster or living crystal states that become locally jammed or clogged by the obstacles. We also find that the system dynamically jams at lower particle densities when the run length is increased. Our results indicate that there is an optimal activity level for transport of run-and-tumble type active matter through quenched disorder and could be important for understanding biological transport in complex environments or for applications of active matter particles in random media.

DOI: 10.1103/PhysRevE.90.012701 PACS number(s): 87.18.Hf, 64.75.Xc, 05.60.Cd, 47.63.Gd

I. INTRODUCTION

There has been tremendous growth in interest in what are termed active matter systems, where the individual units comprising the system undergo self-propulsion [1–3]. Biological examples of such systems include swimming bacteria [4,5], crawling cells [3], and flocking or swarming particles or agents [6]. Nonbiological active matter, such as self-driven colloids [7–10], artificial swimmers [11], and assemblies of self-motile mechanical devices such as bristle bots [12], has been the focus of an increasing number of studies. Active matter systems exhibit a rich variety of behaviors that disappear when the fluctuations experienced by the particles are only equilibrium or thermal in nature. There are different classes of dynamical rules for the motion of self-driven particles. In run-and-tumble dynamics of the type exhibited by some bacteria [4,5], the particle moves in a fixed direction for a period of time before undergoing a tumbling event and changing directions. Active Brownian particles are driven by a motor in a direction that slowly rotates due to a noise term, a dynamics that appears in many self-driven colloidal systems [2,7,10,13–15]. Flocking particles select their direction of motion based on the average swimming direction of their neighbors in a manner captured by the Vicsek model [6]. It was recently shown that active Brownian particle dynamics and the run-and-tumble (RT) dynamics can be mapped into each other and can be considered equivalent [16], whereas Vicsek type flocking models form a separate class.

When collections of sterically interacting particles such as hard disks undergo thermal fluctuations, they form a uniformly dense state; however, when the particles are active and obey RT dynamics there can be a transition to a phase-separated state consisting of high density clusters residing in a low density active gas [10,13–21]. In two-dimensional (2D) systems of monodisperse active disks, the clusters have internal hexagonal or crystalline ordering [10,18,19]. Recent experiments on light-activated self-driven colloidal particles that form such crystalline cluster states revealed that the clusters are highly dynamical, frequently breaking up and reforming, so that the cluster state has been termed a "living crystal" [10]. Similar living crystals have been experimentally observed in other self-driven colloidal systems [19]. The onset of the cluster phase depends both on the particle density and on the activity level, defined as the distance R_l the particles move in a fixed direction during each run in a dilute system.

Studies of active matter have generally focused on systems with a smooth substrate. For example, jamming and glassy effects have been used to connect activity with an effective temperature [14,22–24]. Understanding how active matter particles move in random or complex landscapes is an open question that is relevant to biological systems operating in a complex environment. Possible active matter applications could also require the particles to interact with disordered landscapes. In studies of RT particles interacting with arrays of asymmetric barriers, ratchet effects arise when the activity causes a breaking of detailed balance in the particle-barrier interactions [5,25–29]. Recent studies of particles obeying Vicsek flocking rules without steric particle-particle interactions showed that there is an optimum noise level that maximizes the amount of collective motion, defined as the number of particles that are all swimming in the same direction [30]. Studies of swarming models in disordered environments indicate that disorder can destroy the collective motion phase [31], while a recent study showed that disordered substrates can localize or trap flocking active particles [32]. Since the flocking models are a different class of system from RT models, it would be interesting to understand if an optimal activity level can occur in the RT system.

Here we consider RT particles with steric interactions which undergo a clustering transition at longer R_l when local jamming effects occur. We study particle transport over a disordered substrate in the presence of an external drift force, which could be produced experimentally for active colloids through fluid flow or an electrophoretic current or for bacteria by a chemotactic drift. In the absence of a substrate, the net particle velocity $\langle V_x \rangle$ is determined only by the drift force $\mathbf{F}^D = F_d\hat{\mathbf{x}}$ and is independent of R_l. Particle transport over disordered substrates under an external drift is a very general problem that has been studied in a variety of condensed matter systems including colloids moving over random substrates [33], vortices moving in dirty type II superconductors [34], sliding charge density waves [35], classical charge transport [36], and the motion of magnetic domain walls [37]. In

these systems, the particle transport in the direction of the external drift increases with increasing thermal fluctuations, which diminish the effectiveness of pinning by the substrate. RT particles might be expected to experience significantly reduced pinning by the substrate since, as R_l is increased, the particles would be better able to escape from effective trapping regions; however, in this work we show that this is generally not the case. We find that as the obstacle density increases, $\langle V_x \rangle$ monotonically decreases, and that for fixed obstacle density, $\langle V_x \rangle$ initially increases with R_l before reaching a maximum and then decreasing to zero. This decrease in transport coincides with the formation of large clusters or living crystals of particles due to local jamming effects, which permit an entire cluster to be pinned by a small number of obstacles. Our results show that there is an optimal run length or activity at which maximum transport of the RT particles through disordered media can be achieved. We also demonstrate that the jamming transitions observed in 2D assemblies of nonactive disks [38–41] can be connected to active matter systems and that activity can form a new axis of the jamming phase diagram.

II. SIMULATION

We consider 2D systems of size $L \times L$ with periodic boundary conditions in the x and y directions containing an assembly of N_a active disks with radius r_d that interact with each other via a harmonic repulsion. The dynamics of disk i located at $\mathbf{R}_i$ is obtained by integrating an equation of motion,

$$\eta \frac{d\mathbf{R}_i}{dt} = \mathbf{F}_i^m + \mathbf{F}_i^s + \mathbf{F}_i^b + \mathbf{F}^D, \tag{1}$$

where $\eta = 1.0$ is the damping constant. Under the motor force $\mathbf{F}_i^m$, a particle moves in a fixed direction with a constant velocity F^m/η for a fixed run time τ_r, and at the end of each running time a new running direction is chosen at random. We select F^m such that the particles can never pass through one another or through the obstacles. A single particle in the absence of other particles or obstacles moves a distance $R_l = F^m \tau_r$ in one running time. The steric disk-disk repulsion is modeled as $\mathbf{F}_i^s = \sum_{i \neq j}^{N_a} (2r_d - |\mathbf{r}_{ij}|)\Theta(2r_d - |\mathbf{r}_{ij}|)\hat{\mathbf{r}}_{ij}$, where $\mathbf{r}_{ij} = \mathbf{R}_i - \mathbf{R}_j$, $\hat{\mathbf{r}}_{ij} = \mathbf{r}_{ij}/|\mathbf{r}_{ij}|$, and we take $r_d = 0.5$. The term $\mathbf{F}_i^b$ represents the particle-obstacle interactions, where we model the obstacles as N_p immobile disks that have the same steric interactions as the active disks. The drift force $\mathbf{F}^D = F_d\hat{\mathbf{x}}$ with $F_d = 0.05$. The disk density ϕ is determined by the area covered by all the disks, $\phi = N\pi r_d^2/L^2$, where $N = N_a + N_p$, and the pin density is $\phi_p = N_p\pi r_d^2/L^2$; here, we consider systems with $L = 100$. In the absence of any obstacles or thermal fluctuations, the disks form a hexagonal solid at $\phi_s \approx 0.9$. To measure transport we calculate the average drift velocity $\langle V_x \rangle = (1/N)\sum_{i=1}^{N} \mathbf{v}_i \cdot \hat{\mathbf{x}}$. In the absence of a drift force, $\langle V_x \rangle = 0$, and in the absence of any obstacles, all the particles move with $\langle V_x \rangle = F_d$.

III. RESULTS

We first characterize the onset of clustering in the absence of quenched disorder. To quantify the amount of clustering

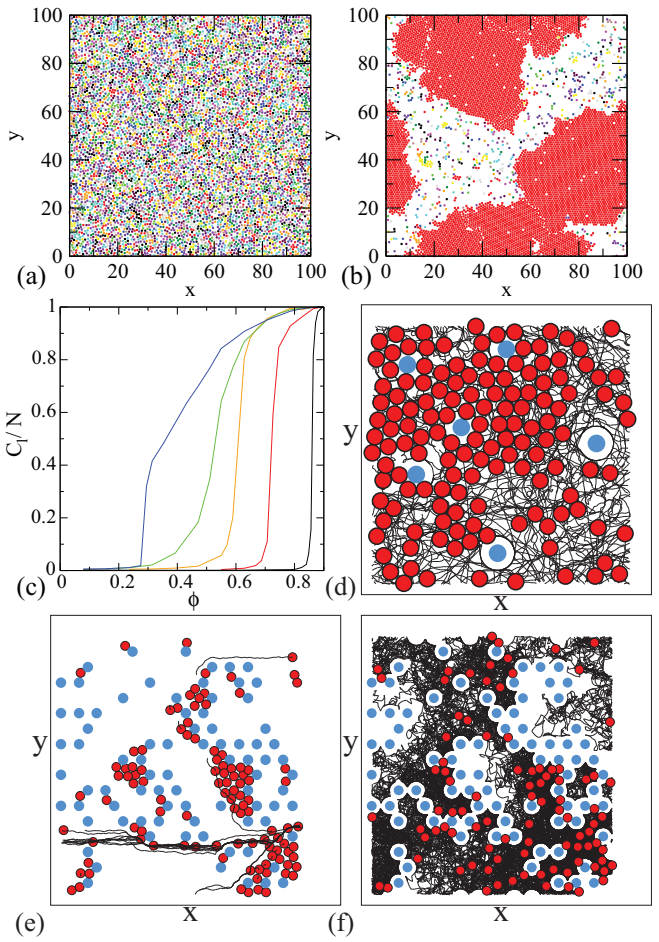

FIG. 1. (Color online) (a),(b) Snapshots of disk positions in an obstacle-free system with $\phi = 0.667$ and $N_p = 0$. (a) Uniform liquid at $R_l = 0.4$. (b) Phase separated state at $R_l = 100$ with a large cluster (red) of local density $\phi \approx 0.9$ surrounded by a low density gas of particles. (c) C_l/N, the fraction of particles in the largest cluster, vs ϕ in the $N_p = 0$ system for $R_l = 40$, 20, 1.4, 0.2, and 0.04, from left to right. The onset of clustering occurs at higher ϕ for decreasing R_l. (d),(e),(f) Positions of pinned disks (light blue circles), active disks (dark red circles), and disk trajectories over a period of time (lines) in small sections of samples with $N_p = 300$ and $\phi_p = 0.0235$. (d) $\phi = 0.667$ and $R_l = 20$. (e) $\phi = 0.188$ and $R_l = 0.004$. (f) $\phi = 0.188$ and $R_l = 0.8$.

present, we utilize a cluster-identification algorithm described in Ref. [42]. In Figs. 1(a) and 1(b) we show the onset of cluster formation at a fixed density of $\phi = 0.667$ when R_l is increased. At $R_l = 0.4$ in Fig. 1(a), there is a uniform liquid phase, while at $R_l = 100$ in Fig. 1(b) the system phase separates into a crystalline hexagonally ordered solid phase with a local density of $\phi = 0.9$ surrounded by a low density gas phase. This behavior is identical to that found in simulations of active Brownian particles at a fixed density when the persistence length is increased [18]. Cluster formation also occurs when ϕ is increased for fixed R_l. In Fig. 1(c) we plot C_l/N, the average fraction of particles in the largest cluster, versus ϕ for systems with $R_l = 0.04$ to 40. At the smallest run length of $R_l = 0.04$, clustering does not occur until the density is well

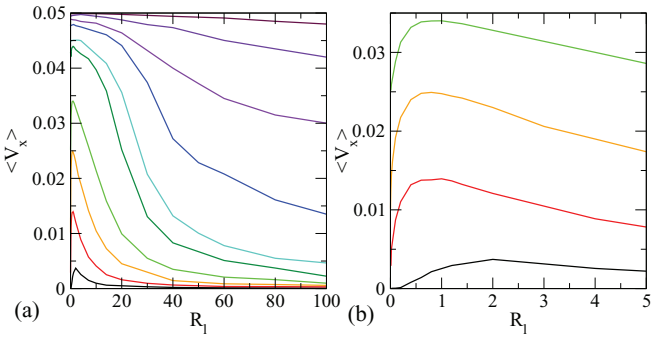

FIG. 2. (Color online) (a) $\langle V_x \rangle$, the average velocity per particle in the drift direction, vs R_l for a system with $\phi = 0.667$ and obstacle density $\phi_p = 0.000\,39, 0.001\,57, 0.004\,72, 0.0785, 0.0157, 0.023\,56, 0.055, 0.0942, 0.014\,13$, and 0.188, from top to bottom. When $R_l > 5.0$, $\langle V_x \rangle$ decreases with increasing R_l. (b) $\langle V_x \rangle$ vs R_l passes through a maximum for all the curves, as shown more clearly in this blow-up of panel (a) for $\phi_p = 0.055, 0.094, 0.1413$, and 0.188, from top to bottom.

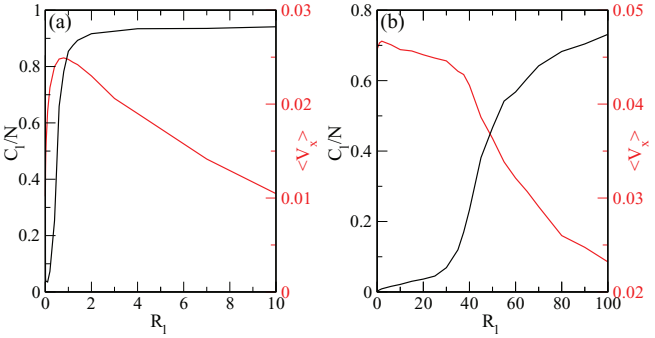

FIG. 3. (Color online) (a) C_l/N (dark curve) and $\langle V_x \rangle$ (light curve) vs R_l for a system with $\phi = 0.667$ and $\phi_p = 0.094$. The drop in $\langle V_x \rangle$ is correlated with the formation of cluster states. (b) The same for a system with $\phi = 0.337$ and $\phi_p = 0.023\,56$.

above $\phi = 0.8$, while for large R_l the onset of clustering shifts to much lower values of ϕ.

We next consider the effect of adding a drift force and N_p obstacles in the form of immobile disks, as illustrated in Fig. 1(d). In Fig. 2(a) we plot a series of transport curves showing $\langle V_x \rangle$ versus R_l at fixed $\phi = 0.667$ and ϕ_p ranging from 0.000 39 to 0.188. For fixed ϕ, Fig. 2(a) shows that increasing ϕ_p monotonically decreases the transport. For any given ϕ_p, the transport initially increases with increasing R_l, reaches an optimal value, and then decreases at larger R_l. In Fig. 2(b) we highlight the transport curves for $\phi_p = 0.055$, 0.094, 0.1413, and 0.188, where the maximum in $\langle V_x \rangle$ occurs near $R_l = 1.0$. The decrease in $\langle V_x \rangle$ at both large and small R_l is correlated with a heterogeneous distribution of particles in the system, due to clogging behind obstacles for small R_l and due to living crystal formation for large R_l. At $\phi_p = 0.188$ in Fig. 2(a), the system completely jams at higher R_l with $\langle V_x \rangle \approx 0$.

In driven systems with quenched disorder, such as superconducting vortices driven over random landscapes [34], increasing the temperature T generally monotonically increases the transport up to a saturation value $\langle V_x \rangle_s$. In our RT system, increasing R_l for small R_l is is similar to increasing the temperature; however, once R_l is large enough for clustering to occur, the particle density becomes inhomogeneous and $\langle V_x \rangle$ drops. We have examined a variety of values of ϕ and ϕ_p and find that in general, for $\phi > 0.4$, when quenched disorder is present the drift velocity is maximized at an optimal value of R_l.

To show that the onset of clustering correlates with the decrease in transport, in Fig. 3(a) we plot $\langle V_x \rangle$ and C_l/N versus R_l for a system with $\phi = 0.667$ and $\phi_p = 0.094$. The decrease in $\langle V_x \rangle$ coincides with an increase in C_l/N, indicating cluster formation. When R_l is small, all of the mobile particles are in the gas phase, and if a particle encounters an obstacle, it has a high probability of quickly changing its swimming direction and moving away from the obstacle. As R_l increases and the system enters the cluster phase, even a single obstacle can pin a cluster since the cluster has transient rigidity. As a result, the moving clusters can become clogged by the obstacles, reducing the transport. Figure 1(d) illustrates the trapping of a high density cluster by obstacles, while the particles in lower density regions remain more mobile. The particles that belong to a cluster become unpinned once the cluster breaks apart. The lifetime of individual clusters increases with increasing R_l and the longer-lived clusters remain clogged for longer periods of time, resulting in a gradual reduction in $\langle V_x \rangle$ with increasing R_l as shown in Fig. 2. For $\phi_p > 0.0785$, in the cluster regime where $\langle V_x \rangle$ decreases with increasing R_l we find $V_x(R_l) \propto R_l^{-\alpha}$, with $\alpha = 1.31 \pm 0.02$, as illustrated in Fig. 4(a). If we fix R_l and vary ϕ_p, Fig. 4(b) shows that for small R_l, $\langle V_x \rangle$ decreases linearly with increasing ϕ_p, while for large R_l the decrease is much more rapid and approximately follows $\langle V_x \rangle \propto 1/\phi_p$. In Fig. 3(b) we plot C_l/N and $\langle V_x \rangle$ vs R_l for a system with $\phi = 0.337$ and $\phi_p = 0.023\,56$. The transport is almost constant at the values of R_l where clustering is absent;

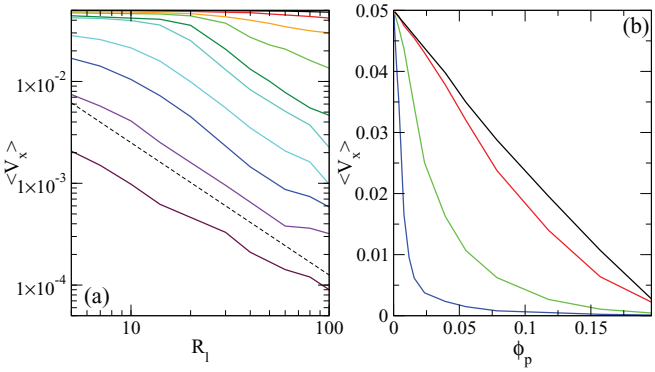

FIG. 4. (Color online) (a) A log-log plot of $\langle V_x \rangle$ vs R_l for systems with $\phi = 0.667$ at $\phi_p = 0.000\,39, 0.001\,57, 0.004\,72, 0.0785, 0.0157, 0.023\,56, 0.055, 0.0942, 0.014\,13$, and 0.188, from top to bottom. The dashed line is a fit to a power law with $V_x(R_l) \propto R_l^{-\alpha}$, with $\alpha = 1.31 \pm 0.02$. (b) $\langle V_x \rangle$ vs ϕ_p at a fixed $\phi = 0.667$ for $R_l = 1.0$, 4.0, 20.0, and 80.0, from top to bottom. At small R_l, $\langle V_x \rangle$ decreases linearly with increasing obstacle density, while for large R_l the decrease is much more rapid and approximately follows $\langle V_x \rangle \propto 1/\phi_p$.

however, at the onset of clustering where C_l/N increases, $\langle V_x \rangle$ begins to drop rapidly.

At low R_l, the drift force can cause individual particles to become trapped behind the obstacles and form locally jammed states even when ϕ is well below the jamming density in a clean system, as illustrated in Fig. 1(e) at $\phi = 0.188$, $\phi_p = 0.0235$, and $R_l = 0.004$ where there is one freely flowing channel but a considerable portion of the particles are trapped. Due to the finite R_l, trapped particles can occasionally escape, as shown in the upper part of Fig. 1(e). As R_l increases, particles can more easily escape from behind the obstacles by moving in directions opposite and transverse to the drift force, and the mobility of the system is enhanced, as illustrated in Fig. 1(f) at $R_l = 0.8$. Thus, increasing the activity by increasing R_l can increase the mobility by reducing the trapping of individual particles; however, at larger R_l, the particles begin clustering into living crystal structures which become locally clogged, causing the mobility to fall at higher R_l.

We next show how the transport is affected by jamming at higher particle density. The jamming concept was originally applied to nonactive particles in the zero-temperature limit, where it was shown that as a function of increasing density the system becomes jammed at ϕ_j, termed point J [38]. In 2D assemblies of bidisperse disks, point J falls at $\phi_j = 0.844$ [39], while for monodisperse disk assemblies the system forms a hexagonal solid at $\phi = 0.9$. Recently it was shown that the addition of quenched disorder to a jamming system decreases the jamming density, where jamming was defined to occur when the drift velocity $\langle V_x \rangle = 0$ under an external applied drive [40]. In the RT system for the nonactive limit of $R_l = 0$, we can obtain a jammed state with $\langle V_x \rangle = 0$ by increasing ϕ for fixed ϕ_p or increasing ϕ_p for fixed ϕ. In Fig. 5(a) we plot $\langle V_x \rangle$ vs R_l for samples with $\phi_p = 0.0942$ at $\phi = 0.667$, 0.746, 0.785, 0.8246, and 0.864. Each curve has an a optimal R_l for transport, and the magnitude of $\langle V_x \rangle$ *decreases* with increasing ϕ. For $\phi > 0.746$, $\langle V_x \rangle = 0$ at $R_l = 0$, corresponding to the jammed phase. For nonzero R_l, the decrease in $\langle V_x \rangle$ with increasing ϕ is due to the formation of clusters which increase in size with increasing ϕ. For moderate to large values of ϕ_p,

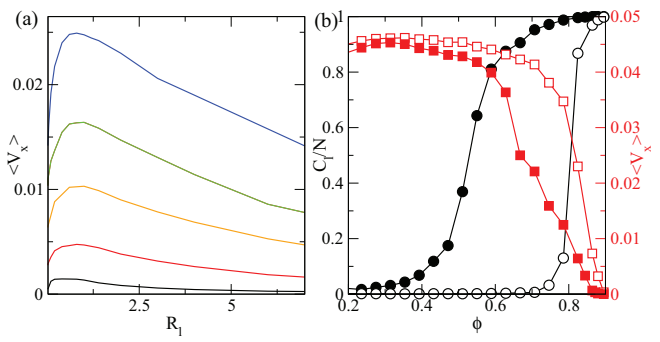

FIG. 5. (Color online) (a) $\langle V_x \rangle$ vs R_l for systems with $\phi_p = 0.0942$ at $\phi = 0.667$, 0.746, 0.785, 0.8246, and 0.864 (from top to bottom) showing the decrease in the transport for increasing ϕ. (b) C_l/N (circles) and $\langle V_x \rangle$ (squares) vs ϕ for samples with $\phi_p = 0.0235$ at $R_l = 0.04$ (open symbols) and $R_l = 20$ (solid symbols) showing the correlation between the onset of clustering and the drop in the transport.

we find that the system reaches the $\langle V_x \rangle = 0$ jammed state if infinite run times are used, so that complete jamming can occur at the limits $R_l = 0$ and $R_l = \infty$. In Fig. 5(b) we plot C_l/N and $\langle V_x \rangle$ versus ϕ for samples with $\phi_p = 0.0235$ at $R_l = 0.04$ and $R_l = 20$. For $R_l = 0.04$, $\langle V_x \rangle$ is constant over most of the range of ϕ but rapidly decreases to a value near zero at $\phi = 0.9$, where we also find a rapid increase in C_l/N. For $R_l = 20$, the onset of clustering occurs at a lower value of ϕ and is also correlated with a drop in $\langle V_x \rangle$. Our results suggest the possibility of adding a new axis to the jamming phase diagram [38] corresponding to the activity R_l, where for large activity there could be another critical jamming point A_j similar to point J.

IV. DISCUSSION

We have shown that an RT active matter model with quenched disorder has an optimal activity level at which transport under a drift force is maximized. In Ref. [30] it was demonstrated that a flocking model with quenched disorder and without steric particle-particle interactions has an optimum noise level at which collective or flocking motion is maximized. The flocking model falls in a very different class of behavior from the RT model, and it is interesting to compare the two results. We measure a flux through our system while in Ref. [30] the tendency for particles to swim in the same direction is measured. These are two very distinct quantities that cannot be mapped onto each other. The decrease in the transport in our system at larger R_l is due to local jamming effects caused by steric interactions between the particles. These effects are absent in the flocking model, which instead has a transition from coordinated to uncoordinated swimming as a function of noise. Thus, the optimal activity level and optimum noise level observations are distinct and are produced by quite different physical effects.

We find that increasing the run length or particle density can substantially decrease the mobility of the RT particles through a substrate due to cluster formation and local clogging. In order to avoid such clogging effects, new types of motion rules could be devised for the RT particles, such as having the particles reverse or randomize their swimming direction if they become immobilized by an obstacle or trapped in a cluster. It would be interesting to explore whether biologically relevant active matter such as swimming organisms have evolved methods to avoid self-clogging.

V. SUMMARY

We have examined the transport of RT active matter particles driven through quenched disordered environments. Unlike thermalized particles driven over random disorder, where previous studies have shown that the transport is generally increased when the thermal fluctuations increase, we find that for active matter the transport first increases and then decreases as the activity level or running length increases due to the formation of living crystals that can be locally jammed or clogged. The system becomes effectively jammed at lower densities as the run length increases, suggesting that activity could form a new axis of the jamming phase diagram.

Since recent theoretical work has shown that RT dynamics and active Brownian motion can be mapped to each other [38], our results can be generalized to other active systems driven over quenched disorder.

ACKNOWLEDGMENTS

We thank L. Lopatina for useful discussions. This work was carried out under the auspices of the NNSA of the U.S. DoE at LANL under Contract No. DE-AC52-06NA25396.

[1] S. Ramaswamy, Annu. Rev. Condens. Matter Phys. **1**, 323 (2010).
[2] B. ten Hagen, S. van Teeffelwn, and H. Löwen, J. Phys.: Condens. Matter **23**, 194119 (2011); H. H. Wensink and H. Löwen, *ibid.* **24**, 464130 (2012); P. Romanczuk, M. Bär, W. Ebeling, B. Lindner, and L. Schimansky-Geier, Eur. Phys. J. Spec. Top. **202**, 1 (2012).
[3] M. C. Marchetti, J. F. Joanny, S. Ramaswamy, T. B. Liverpool, J. Prost, M. Rao, and R. A. Simha, Rev. Mod. Phys. **85**, 1143 (2013).
[4] H. C. Berg, *Random Walks in Biology* (Princeton University Press, Princeton, NJ, 1983).
[5] P. Galajda, J. Keymer, P. Chaikin, and R. Austin, J. Bacteriol. **189**, 8704 (2007).
[6] T. Vicsek, A. Czirók, E. Ben-Jacob, I. Cohen, and O. Shochet, Phys. Rev. Lett. **75**, 1226 (1995); H. Chaté, F. Ginelli, G. Grégoire, F. Peruani, and F. Raynaud, Eur. Phys. J. B **64**, 451 (2008).
[7] W. F. Paxton, K. C. Kistler, C. C. Olmeda, A. Sen, S. K. St. Angelo, Y. Y. Cao, T. E. Mallouk, P. E. Lammert, and V. H. Crespi, J. Am. Chem. Soc. **126**, 13424 (2004); J. R. Howse, R. A. L. Jones, A. J. Ryan, T. Gough, R. Vafabakhsh, and R. Golestanian, Phys. Rev. Lett. **99**, 048102 (2007).
[8] R. Golestanian, Phys. Rev. Lett. **102**, 188305 (2009).
[9] G. Volpe, I. Buttinoni, D. Vogt, H.-J. Kummerer, and C. Bechinger, Soft Matter **7**, 8810 (2011).
[10] J. Palacci, S. Sacanna, A. P. Steinberg, D. J. Pine, and P. M. Chaikin, Science **339**, 936 (2013).
[11] R. Dreyfus, J. Baudry, M. L. Roper, M. Fermigier, H. A. Stone, and J. Bibette, Nature (London) **437**, 862 (2005).
[12] L. Giomi, N. Hawley-Weld, and L. Mahadevan, Proc. R. Soc. London, Ser. A **469**, 20120637 (2013).
[13] J. Bialké, T. Speck, and H. Löwen, Phys. Rev. Lett. **108**, 168301 (2012).
[14] S. Henkes, Y. Fily, and M. C. Marchetti, Phys. Rev. E **84**, 040301 (2011).
[15] Y. Fily and M. C. Marchetti, Phys. Rev. Lett. **108**, 235702 (2012).
[16] M. E. Cates and J. Tailleur, Europhys. Lett. **101**, 20010 (2013).
[17] I. Theurkauff, C. Cottin-Bizonne, J. Palacci, C. Ybert, and L. Bocquet, Phys. Rev. Lett. **108**, 268303 (2012).
[18] G. S. Redner, M. F. Hagan, and A. Baskaran, Phys. Rev. Lett. **110**, 055701 (2013).
[19] I. Buttinoni, J. Bialké, F. Kümmel, H. Löwen, C. Bechinger, and T. Speck, Phys. Rev. Lett. **110**, 238301 (2013).
[20] J. Stenhammar, A. Tiribocchi, R. J. Allen, D. Marenduzzo, and M. E. Cates, Phys. Rev. Lett. **111**, 145702 (2013).
[21] B. M. Mognetti, A. Saric, S. Angioletti-Uberti, A. Cacciuto, C. Valeriani, and D. Frenkel, Phys. Rev. Lett. **111**, 245702 (2013).
[22] Y. Fily, S. Henkes, and M. C. Marchetti, Soft Matter **10**, 2132 (2014).
[23] R. Ni, M. A. C. Stuart, and M. Dijkstra, Nat. Commun. **4**, 2704 (2013).
[24] L. Berthier and J. Kurchan, Nat. Phys. **9**, 310 (2013); L. Berthier, Phys. Rev. Lett. **112**, 220602 (2014).
[25] M. B. Wan, C. J. Olson Reichhardt, Z. Nussinov, and C. Reichhardt, Phys. Rev. Lett. **101**, 018102 (2008); C. Reichhardt and C. J. Olson Reichhardt, Phys. Rev. E **88**, 062310 (2013).
[26] J. Tailleur and M. E. Cates, Europhys. Lett. **86**, 60002 (2009).
[27] J. A. Drocco, C. J. Olson Reichhardt, and C. Reichhardt, Phys. Rev. E **85**, 056102 (2012).
[28] M. E. Cates, Rep. Prog. Phys. **75**, 042601 (2012).
[29] L. Angelani, A. Costanzo, and R. Di Leonardo, Europhys. Lett. **96**, 68002 (2011); V. Kantsler, J. Dunkel, M. Polin, and R. E. Goldstein, Proc. Natl. Acad. Sci. USA **110**, 1187 (2013); I. Berdakin, Y. Jeyaram, V. V. Moshchalkov, L. Venken, S. Dierckx, S. J. Vanderleyden, A. V. Silhanek, C. A. Condat, and V. I. Marconi, Phys. Rev. E **87**, 052702 (2013).
[30] O. Chepizhko, E. G. Altmann, and F. Peruani, Phys. Rev. Lett. **110**, 238101 (2013).
[31] D. A. Quint and A. Gopinathan, arXiv:1302.6564.
[32] O. Chepizhko and F. Peruani, Phys. Rev. Lett. **111**, 160604 (2013).
[33] C. Reichhardt and C. J. Olson, Phys. Rev. Lett. **89**, 078301 (2002); A. Pertsinidis and X. S. Ling, *ibid.* **100**, 028303 (2008); P. Tierno, *ibid.* **109**, 198304 (2012).
[34] G. Blatter, M. V. Feigelman, V. B. Geshkenbein, A. I. Larkin, and V. M. Vinokur, Rev. Mod. Phys. **66**, 1125 (1994).
[35] G. Grüner, Rev. Mod. Phys. **60**, 1129 (1988).
[36] F. I. B. Williams, P. A. Wright, R. G. Clark, E. Y. Andrei, G. Deville, D. C. Glattli, O. Probst, B. Etienne, C. Dorin, C. T. Foxon, and J. J. Harris, Phys. Rev. Lett. **66**, 3285 (1991); H.-W. Jiang, H. L. Stormer, D. C. Tsui, L. N. Pfeiffer, and K. W. West, Phys. Rev. B **44**, 8107 (1991).
[37] S. Lemerle, J. Ferré, C. Chappert, V. Mathet, T. Giamarchi, and P. Le Doussal, Phys. Rev. Lett. **80**, 849 (1998); P. J. Metaxas, J. P. Jamet, A. Mougin, M. Cormier, J. Ferré, V. Baltz, B. Rodmacq, B. Dieny, and R. L. Stamps, *ibid.* **99**, 217208 (2007).
[38] A. J. Liu and S. R. Nagel, Nature (London) **396**, 21 (1998).
[39] C. S. O'Hern, L. E. Silbert, A. J. Liu, and S. R. Nagel, Phys. Rev. E **68**, 011306 (2003); J. A. Drocco, M. B. Hastings, C. J. Olson Reichhardt, and C. Reichhardt, Phys. Rev. Lett. **95**, 088001 (2005).
[40] C. J. Olson Reichhardt, E. Groopman, Z. Nussinov, and C. Reichhardt, Phys. Rev. E **86**, 061301 (2012).
[41] C. Reichhardt and C. J. Olson Reichhardt, Soft Matter **10**, 2932 (2014).
[42] S. Luding and H. J. Herrmann, Chaos **9**, 673 (1999).